Reduction of Dental Filling Metallic Artifacts in CT-Based Attenuation Correction of PET Data Using Weighted Virtual Sinograms

M. Abdoli, M.R. Ay, *Member, IEEE*, A. Ahmadian, *Senior Member, IEEE* and H. Zaidi, *Senior Member, IEEE*

***Abstract*– The streak artifacts caused by dental fillings are known to generate artifacts in attenuation maps thus leading to overestimation/underestimation of tracer uptake in resulting PET images. Correction of these artifacts is therefore mandatory to achieve accurate attenuation maps to be used by the CT-based attenuation correction procedure. Our group recently proposed a metal artifact reduction method using the virtual sinogram concept. In spite of the satisfactory results obtained on phantom studies, the algorithm was suffering from slight imperfections such as discontinuity of corrected sinogram bins along the second dimension of the sinogram matrix (i.e. the one sampling angular positions) and an evident difference between corrected and non-affected sinogram bins, especially when the number of affected bins in one column of the sinogram matrix is noticeable. The purpose of this study is to present an improved method allowing to overcome the above mentioned limitations. The proposed method enhances the corrected sinogram using weighted values of the influenced bins in the corrected and non-corrected sinograms, and weighted values of the sinogram bins in the neighboring column of the sinogram matrix. The optimum weighting factors associated with the three data sets mentioned above (α, β and γ) were determined by assessing different combinations of these factors having values falling in the range [0.1-0.9] and statistical analysis of the images of 10 patients with dental fillings. The optimum combination achieved is α=0.3, β=0.6 and γ=0.1. The results reveal that the corrected CT images and attenuation maps preserve more detail especially in regions adjacent to metallic objects whereas the original method suffered from eliminating relevant anatomical details. It was concluded that the proposed MAR method using weighted virtual sinograms improves the quality of clinical CT studies thus allowing the achievement of more accurate attenuation correction of PET data.**

I. Introduction

Dual modality PET/CT imaging is considered as one of the revolutionary technical advances that overcome the limitations of single modality imaging [1]. Attenuation correction is a necessary step to obtain clinically reliable PET emission data. This process is performed using attenuation maps (μmaps) representing the spatial distribution of linear attenuation coefficients (LACs) at 511 keV. Since the intensity of CT image voxels is related to electronic density and thus the LAC of the corresponding tissue, they can be used to generate μmaps at the corresponding photon energy. The use of CT-based attenuation correction (CTAC) allows decreasing the overall scanning time and creating a noise-free μmap. However, the presence of streak artifacts caused by metallic inserts, such as dental fillings, is known to generate artifacts in μmaps, thus leading to overestimation/underestimation of tracer uptake in resulting PET images [2,3]. As a consequence, correction of these artifacts is mandatory to achieve accurate attenuation maps to be used by the CTAC procedure.

Metal artifact reduction (MAR) methods can be divided into image-based and sinogram-based techniques. In the first group, the correction is implemented in sinogram space. Linear interpolation of the missing data is one popular techniques belonging to this class of methods [4]. Since the difference between metallic objects and other tissues' CT numbers is considerable, simple thresholding can be used for segmenting metallic objects. The extracted image is forward projected to determine the projections in the sinogram space which are affected by metallic objects. These projections are then replaced by linear interpolation of other projections in the same projection angle. Finally, the corrected image is obtained from the reconstruction of the corrected sinogram through application of the inverse Radon transform. Cubic interpolation of unaffected projections is another way of replacing the missing projections [5].

Replacing missing projections by their unaffected correspondence is another method belonging to this category [6]. In this method, instead of using an interpolation algorithm, missing projections are replaced by their corresponding unaffected projection, i.e. the opposite angular position in spiral scanning or the same angular position of the next slice in step scanning. The second category of methods manipulates directly the images using image processing

This work was supported by Tehran University of Medical Sciences under grant 132/494 and the Swiss National Science Foundation under grant 3152A0-102143.

Mehrsima Abdoli is with the Department of Medical Physics and Biomedical Engineering, Tehran University of Medical Sciences, Tehran, Iran and Research Center for Science and Technology in Medicine, Tehran, Iran, and Department of Nuclear Medicine and Molecular Imaging, University Medical Center Groningen, University of Groningen, Groningen, The Netherlands (e-mail: mehrsima.abdoli@gmail.com).

Mohammad Reza Ay is with the Department of Medical Physics and Biomedical Engineering, Tehran University of Medical Sciences, Tehran, Iran and Research Center for Science and Technology in Medicine, Tehran, Iran, and Research Institute for Nuclear Medicine, Tehran University of Medical Sciences, Tehran, Iran (e-mail: mohammadreza_ay@tums.ac.ir).

Alireza Ahmadian is with the Department of Medical Physics and Biomedical Engineering, Tehran University of Medical Sciences, Tehran, Iran and Research Center for Science and Technology in Medicine, Tehran, Iran (e-mail: ahmadian@sina.tums.ac.ir)

Habib Zaidi is with the Division of Nuclear Medicine, Geneva University Hospital, CH-1211 Geneva, Switzerland (e-mail: habib.zaidi@hcuge.ch).

techniques such as iterative deblurring [7], segmentation [8] or knowledge-based methods [9]. Although sinogram-based methods are more accurate, they involve the manipulation of raw projection data consisting of huge encrypted files. To overcome the above mentioned issues, we recently proposed a technique using the concept of virtual sinograms [10]. A virtual sinogram is produced by forward projection of reconstructed CT images in DICOM format. In this method, the projection data affected by metallic objects are first detected in the sinogram space through segmentation of metallic implants in the CT image followed by forward projection of the metal-only image. Thereafter, the extracted sinogram bins are replaced by interpolated values of adjacent bins using the spline interpolation technique. In spite of the satisfactory results obtained on phantom studies, the algorithm was suffering from slight imperfections owing to the fact that following interpolation of the missed bins along one dimension of the virtual sinogram, a discontinuity appeared along the second dimension. Furthermore, when the number of affected bins in one column of the sinogram matrix increases, the value of the interpolated bins will have an obvious difference with the non-affected bins, which is due to the inefficiency of interpolation algorithms in such cases. These imperfections mainly affect clinical data where the images consist of more complex tissue distributions compared to experimental phantoms. The purpose of this study is to present an improved method allowing to overcome the above mentioned limitations and to validate it using clinical CT images presenting with dental fillings, which are used for attenuation correction of PET data.

II. Materials and Methods

Although the virtual sinogram-based MAR algorithm is a suitable approach for reduction of streak artifacts in simple-structured objects, it exemplifies some flaws when using real clinical data containing complex shapes and structures. This suggests that the method requires some improvement so that it can be applied in clinical studies.

The proposed method enhances the corrected sinogram using weighted values of the influenced bins in the corrected and uncorrected sinograms, as well as the neighboring column of the sinogram matrix. Since the intensity of a projection passing through a metallic object reflects a line of response (LOR), it includes both correct and incorrect data. The correct data pertain to a segment of the LOR passing through biological tissues other than the metallic object whereas the incorrect data pertain to the remaining segment of the LOR. Therefore, a weighted proportion of the missed projections can be allocated to the final intensity of these projections. Moreover, the adjacent columns in the sinogram matrix represent the projections obtained from two slightly different angular positions of the x-ray tube. That is, they contain data of approximately the same tissues. As a consequence, sharing a weighted value of the adjacent sinogram bins is not irrelevant to diminish the discontinuity of the corrected sinogram.

In the first step, the algorithm finds a column of the corrected sinogram matrix which has the minimum difference between the interpolated and non-affected bins. This column is considered as the starting point of the improvement procedure (*co*). To do so, we need to define the equation to calculate the error of each column (*c*). Thereafter, the column with the least error can be recognized. Consider the sinogram symbolized by *S* as a matrix with dimension *m*×*n*. Since the projections pertaining to a specific object form a sinus shape in the sinogram matrix, the missed projections can be supposed to form a shape similar to figure 1. The following equation calculates the mentioned error for c_1^{th} column:

$$\varepsilon(c_1)=\frac{\left|S(r_1-1,c_1)-\frac{\sum_{i=r_1}^{r_2}S(i,c_1)}{r_2-r_1+1}\right|+\left|S(r_2+1,c_1)-\frac{\sum_{i=r_1}^{r_2}S(i,c_1)}{r_2-r_1+1}\right|}{2} \quad (1)$$

where ε is the error of the interpolated sinogram bins in comparison with non-affected bins in the same column and r_1 and r_2 represent the higher and lower indices of missed sinogram bins in each column (figure 1).

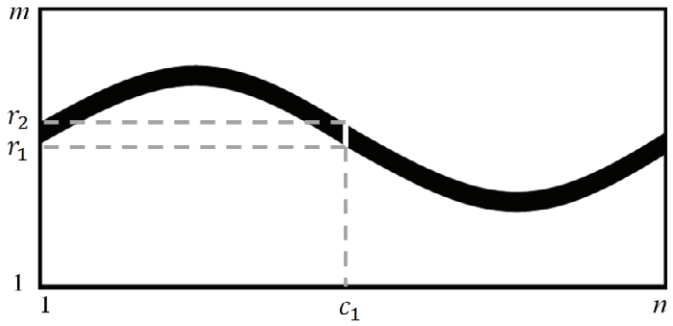

Figure 1. Schematic view of a sinogram. The sinus-shape part represents the interpolated sinogram bins.

In the second step, for each column on the right side of the starting point, the final estimates of the affected bins are determined using the following equation:

$$S_{improved}(r,c)= \quad (2)$$

$$\begin{cases}\alpha\, S_{main}(r,c)+\beta\, S_{corrected}(r,c)+\gamma\dfrac{\sum_{i=r_1}^{r_2}S_{improved}(i,c-1)}{r_2-r_1+1} & c>c_o\\ \alpha\, S_{main}(r,c)+\beta\, S_{corrected}(r,c)+\gamma\dfrac{\sum_{i=r_1}^{r_2}S_{improved}(i,c+1)}{r_2-r_1+1} & c<c_o\end{cases}$$

where $S_{improved}$ is the improved sinogram, S_{main} is the uncorrected sinogram, $S_{corrected}$ is the corrected sinogram using our technique [10], *r* and *c* represent the rows and columns of the sinogram matrices, r_1 and r_2 are the lowest and highest affected rows in each column, and α, β and γ are the weighting factors assigned to S_{main}, $S_{corrected}$ and $S_{improved}$, respectively. Different combinations of these weighing factors having values in range [0.1-0.9] were examined to find the optimum combination. For each combination, the corrected CT image and the corresponding μmap were generated.

Three steps are performed to produce the μmap from the corrected CT images. The first step consists in equalizing the size of the CT and PET images. This is achieved by down-sampling the corrected CT images by a factor of four. The linear attenuation coefficient measured with CT is calculated at the x-ray effective energy rather than at 511 keV. It is therefore necessary to convert linear attenuation coefficients of the CT scan to those corresponding to 511 keV. In this work, a bilinear calibration curve is used for energy conversion which is utilized by most commercial PET/CT scanners. The last step consists in matching the spatial resolution of the CT and PET images. A Gaussian filter with an appropriate kernel size is applied to the μmap to achieve this goal.

The algorithm was applied to CT images of 10 patients presenting with dental fillings. The images were acquired on the GE LightSpeed VCT clinical 64-slice scanner, (General Electric Healthcare Technologies, Waukesha, WI). The generated μmaps were analyzed both qualitatively and quantitatively to evaluate the performance of the algorithm.

III. Results

The μmaps of 10 clinical studies with dental fillings were first visually assessed in order to select the μmaps which contain the least amount of artifacts and most relevant details in regions adjacent to metallic objects. Thereafter, the selected μmaps were quantitatively analyzed to determine the μmap resulting in LACs closest to their corresponding theoretical estimates. The quantitative analysis was performed by defining 50 ROIs on the regions of μmaps corresponding to soft tissue where the theoretical value of the LAC at 511 keV is 0.096 cm^{-1}. The results revealed that for all data sets, there is a unique combination of weighting factors which generates the best results. The optimum combination found is α=0.3, β=0.6 and γ=0.1. This suggests that the corrected sinogram must have the highest contribution, and the adjacent columns must have the least proportion in the final sinogram. Table 1 summarizes the results of paired t-test statistical analysis for the μmaps of 10 patients included in this study. Figure 2 illustrates the uncorrected, corrected and improved sinograms for one typical clinical study. It can be observed that the improved algorithm allows the removal to some extent of the discontinuities in the corrected sinogram. The CT image and μmap of two patients are presented in figures 3 and 4, respectively. As expected, the improved images and μmaps preserve more details especially in regions adjacent to metallic objects, whereas noticeable details of the images are eliminated when using the original techniques [10].

Table 1. Summary of paired t-test statistical analysis of μmaps of 10 patients with dental fillings.

Patients	μmaps					
	Uncorrected		Corrected with virtual sinogram method		Corrected with weighted virtual sinogram method	
	Mean LAC	P-Value	Mean LAC	P-Value	Mean LAC	P-Value
1	0.101	0.0672	0.092	0.050	0.090	0.253
2	0.113	<0.005	0.092	<0.01	0.089	0.286
3	0.110	<0.005	0.091	0.099	0.090	0.271
4	0.108	<0.05	0.092	<0.05	0.090	0.211
5	0.109	<0.05	0.092	0.058	0.090	0.152
6	0.111	<0.01	0.093	0.055	0.090	0.109
7	0.112	<0.005	0.094	<0.005	0.091	0.551
8	0.109	<0.01	0.091	0.056	0.090	0.371
9	0.110	<0.05	0.091	0.127	0.090	0.423
10	0.110	<0.01	0.091	0.104	0.090	0.352

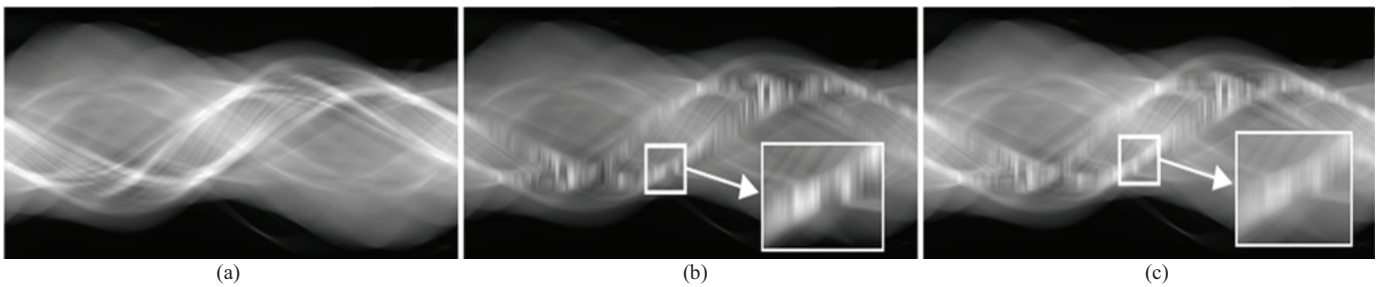

(a) (b) (c)

Figure 2. Sinograms of the CT image of a clinical study: (a) uncorrected sinogram, (b) sinogram corrected using the virtual sinogram method, and (c) sinogram corrected using the weighted virtual sinogram method. Note the continuity of the corrected sinogram shown in (c).

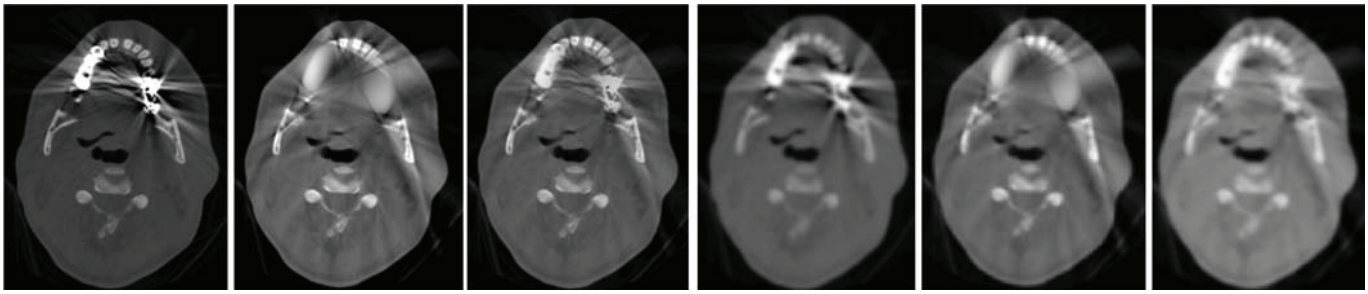

(a) (b) (c) (d) (e) (f)

Figure 3. (a-c) Clinical CT images of one patient reconstructed using the uncorrected, corrected using the virtual sinogram method and corrected using the weighted virtual sinogram method, respectively; (d-f) the corresponding μmaps.

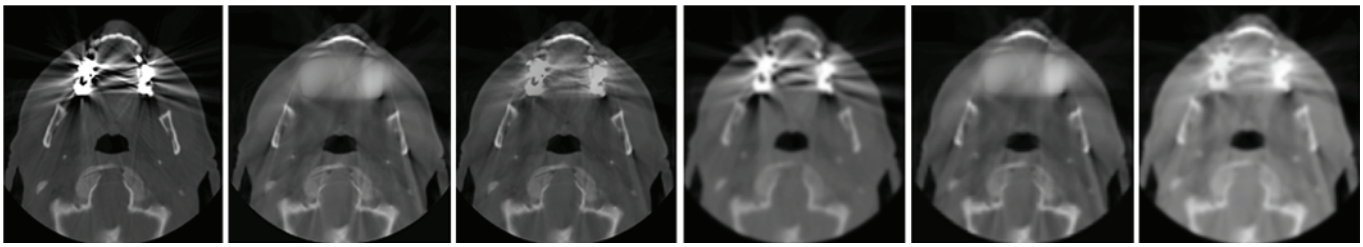

(a) (b) (c) (d) (e) (f)

Figure 4. (a-c) Clinical CT images of another patient reconstructed using the uncorrected, corrected using the virtual sinogram method and corrected using the weighted virtual sinogram method, respectively; (d-f) the corresponding μmaps.

IV. Discussion

The proposed method can be used to generate attenuation maps suitable for attenuation correction of PET data thus providing a convenient method to correct for the presence of metal artifacts caused by dental fillings without the need to use the encrypted raw data. Although the quantitative analysis shows a slight statistically significant difference between the LAC estimates of the corrected μmaps and their corresponding theoretical values for few studies when using the original method, no significant statistical difference is observed when using the proposed improved technique. Figure 2 shows the effect of the proposed method on discontinuities produced in the corrected sinogram. The considerable discontinuities displayed in figure 2(b) are smoothed to an acceptable degree in figure 2(c) which confirms that the improved method is able to obviate the imperfections of the previous method. As illustrated in figures 3 and 4, the missing data in figures (b)-(e) are well restored in figures (c)-(f). It appears that the proposed MAR method using weighted virtual sinograms improves the quality of clinical CT studies thus allowing the achievement of more accurate attenuation correction of PET data. The algorithm is still being refined using optimization algorithms (genetic algorithms) to optimize the weighting factors. Further validation in a clinical setting using a larger clinical PET/CT database is also ongoing.

V. Conclusion

In this study, a new approach was proposed to reduce dental filling artifacts on CT images used in CTAC of PET emission data. The statistical analysis performed on the results of the algorithm reveal that, in comparison with the non-weighted virtual sinogram method, this novel approach results in more reliable attenuation maps thus allowing the achievement of more accurate attenuation correction of PET emission data.

References

[1] DW. Townsend (2008) "Multimodality imaging of structure and function" Phys Med Biol. 53:R1-R39.

[2] EM. Kamel, C. Burger, A. Buck, GK. Schulthess, GW. Goerres (2003) "Impact of metallic dental implants on CT-based attenuation correction in a combined PET/CT scanner" Eur Radiol. 13: 724-728.

[3] C. Lemmens, M-L. Montandon, J. Nuyts, O. Ratib, P. Dupont, H. Zaidi (2008) "Impact of metal artefacts due to EEG electrodes in brain PET/CT imaging" Phys Med Biol. 53: 4417-4429.

[4] W. Kalender, R. Hebel, J. Ebersberger (1987) "Reduction of CT artifacts caused by metallic implants" Radiology. 164: 576-577.

[5] M. Bazalova, L. Beaulieu, S. Palefsky, F. Verhaegen (2007) "Correction of CT artifacts and its influence on Monte Carlo dose calculation." Med. Phys 34(6):2119-2132.

[6] M. Yazdi, L. Beaulieu (2006) "A novel approach for reducing metal artifacts due to metallic dental implants" IEEE Nucl. Sci. Symp. Conf. Rec. 4:2260-2263.

[7] G. Wang, DL. Snyder, JA. O'Sullivan, MW. Vannier (1996) "Iterative deblurring for CT metal artifact reduction" IEEE Trans Med Imaging. 15: 657-664.

[8] S. Mirzaei, M. Guerchaft, C. Bonnier, P. Knoll, M. Doat, P. Braeutigam (2005) "Use of segmented CT transmission map to avoid metal artifacts in PET images by a PET-CT device" BMC Nucl Med. 5:3.

[9] JA. Kennedy, O. Israel, A. Frenkel, R. Bar-Shalom, H. Azhari (2007) "The reduction of artifacts due to metal hip implants in CT-attenuation corrected PET images from hybrid PET/CT scanners" Med Biol Eng Comput. 45: 553-562.

[10] M. Abdoli, MR. Ay, A. Ahmadian, H. Zaidi (2009) "A virtual sinogram method to reduce dental metallic implant artefacts in CT-based attenuation correction for PET" Nucl. Med. Comm. 30: *in press*